Multiphase materials with lignin: 1. Blends of hydroxypropyl lignin with poly(methyl methacrylate)

Scott L. Ciemniecki and Wolfgang G. Glasser
Department of Forest Products, and Polymer Materials and Interfaces Laboratory, Virginia Tech, Blacksburg, VA 24061, USA
(Received 24 August 1987; revised 26 October 1987; accepted 18 November 1987)

Polymer blends consisting of hydroxypropyl lignin (HPL) and poly(methyl methacrylate) (PMMA) were prepared by injection moulding and by solution casting (tetrahydrofuran and chloroform). Blend morphology and material properties were determined by scanning electron microscopy, differential scanning calorimetry, dynamic mechanical thermal analysis and tensile testing. Results were interpreted in relation to HPL content, HPL molecular weight and method of preparation. All blends produced two-phase materials with morphology varying with method of preparation and HPL content. A surprising degree of compatibility was revealed by thermal analysis (differential scanning calorimetry and dynamic mechanical thermal analysis). The behaviour suggests significant plasticization or antiplasticization for all blends. Even the highly phase-separated solution-cast blends showed single T_g values at all HPL contents. These results were explained with transitional smearing, and with some degree of polymer–polymer interaction. The addition of HPL to PMMA was found to cause an increase in modulus and a decrease in ultimate properties. Blends prepared by injection moulding had consistently better material properties than those prepared by solution casting.

(Keywords: lignin; lignin derivatives; plasticization; thermal analysis; dynamic mechanical analysis)

INTRODUCTION

Interest in polymer blends has been rising because blending is seen as an inexpensive method for the modification of polymer properties[1-3]. This is governed by the miscibility or compatibility of the individual blend components. Two polymers are often termed 'miscible' if they form a single, homogeneous phase as determined by an optical or thermal method, and if intimate mixing is achieved on a molecular scale. On the other hand 'compatibility', being more of a commercial term, indicates the usefulness of a blend. Thus, immiscible blends do in certain cases exhibit good mechanical properties and are said to be mechanically compatible[4]. Mechanical compatibility in immiscible blends is generally related to good interfacial adhesion between the phases of the blend constituents. A number of immiscible but compatible blends have drawn considerable commercial interest in recent years. These include bisphenol A polycarbonate/poly(butylene terephthalate) (PC/PBT)[5], poly(vinyl chloride)/acrylonitrile–butadiene–styrene terpolymer (PVC/ABS)[6,7] and poly(vinyl chloride)/poly(methyl methacrylate) (PVC/PMMA) blends[5]. PVC/PMMA blends combine the good flammability resistance of PVC and the higher T_g of PMMA relative to PVC. The blends exhibit higher notched impact strength than either of the blend components. PMMA also improves the thermoforming characteristics of PVC. The combination of these improved properties has allowed PVC/PMMA blends to be used in specific applications such as seat backs, aircraft interior components and industrial wall panelling[5].

In miscible systems, specific interactions that occur between components will increase the overall entanglement of the network structure, thereby creating mechanical compatibility. The blend of polystyrene and poly(2,6-dimethyl-1,4-phenylene oxide) (PS/PPO)[8] is miscible at any composition range and hence blends of any desirable T_g can be obtained by simply varying the composition of the constituents. Miscibility between PS and PPO was reported to be due (among other things) to specific interaction of the phenylene group of PPO and the phenyl group of PS[9].

Two polymers may form an immiscible blend, a miscible blend, or an intermediate. Whether a polymer pair belongs to one or the other category depends primarily on three parameters: (1) solubility parameter, (2) molecular weight and (3) specific interactions between the polymers[10]. The solubility parameter is a measure of the cohesion of the material or the strength of molecular attraction. The effects of molecular weight on miscibility are based on the Flory–Huggins theory, which indicates that the entropy gained on mixing polymers is inversely related to their number-average size[11]. Thus a particular polymer mixture can be made more miscible by reducing the molecular weight of one or both components.

This study deals with the evaluation of engineering materials from lignin by blending hydroxypropyl lignin (HPL) with PMMA. The effects of molecular weight and specific interactions on blend morphology and properties are to be described by optical (i.e. scanning electron microscopy, s.e.m.), thermal (i.e. differential scanning calorimetry, d.s.c., and dynamic mechanical thermal analysis, d.m.t.a.), and mechanical (i.e. tensile testing) techniques.

0032-3861/88/061021-09$03.00

MATERIALS

Kraft lignin

A commercially available kraft lignin (Indulin-AT from Westvaco Corp., Charleston, South Carolina) was used in this study. This originated from the spent pulping liquor of a (mostly) pine-based kraft process.

Hydroxypropyl lignin (HPL)

Kraft lignin was reacted with propylene oxide using a procedure described previously[12]. The isolated reaction product had a hydroxy content of 6.5% (by titration) and a glass transition temperature (T_g) of 63.5°C (by d.s.c.).

Poly(methyl methacrylate) (PMMA)

An atactic PMMA with a T_g of 110°C and an intrinsic viscosity of 1.4 was obtained from Scientific Polymer Products, Inc.

METHODS

Fractionation of HPL

Fractionation of HPL (see ref. 13) employed 2% (by weight) acetone solutions, from which three fractions were precipitated by the addition of increasing amounts of hexane. The material remaining in solution at an acetone/hexane ratio of 0.8 was isolated by solvent evaporation, and it yielded the 'low MW' fraction. The precipitate was dried and redissolved in acetone to give a 2% solution. The precipitation was repeated with a larger hexane fraction, and this produced a 'medium MW' fraction (dissolved), and a 'high MW' fraction (precipitated).

Solution casting

Separate 10% (w/w) solutions of each component were prepared using a tetrahydrofuran (THF), a hydrogen-bonding solvent, and chloroform, a non-hydrogen-bonding solvent, as solvents. The solutions were mixed together, and they were allowed to stir at room temperature overnight. This solution was poured into Teflon moulds and the solvent was allowed to evaporate slowly at room temperature for 2 days. The resulting films were dried in a vacuum oven at 70°C for a week and then stored in a desiccator containing P_2O_5.

Injection moulding

The proper weight per cent of each polymer component was weighed out separately and mixed by mortar and pestle before being injection moulded using a 'mini-Max Molder' by Custom Scientific Instruments[14]. Approximately 0.5 g of material was placed in the stator cup heater, which was set at 230°C. The sample was stirred for 1 min and then injected into a dog-bone mould.

Characterization of HPL fractions

Gel permeation chromatography. Number-average (M_n) and weight-average (M_w) molecular weights were determined by gel permeation chromatography (g.p.c.) in dimethylformamide (DMF)/LiBr on Altex μ-Spherogel columns with pore sizes of 500, 1000, 10000 and 100000 Å. The system was calibrated with polystyrene standards above 25000 daltons, and with lignin-like model compounds below 1000 daltons[13].

Vapour pressure osmometry. Number-average molecular weight was also determined by vapour pressure osmometry (v.p.o.) using a Knauer Dampfdruck Osmometer. Benzil was used for calibration, and dilutions ranged from 0.02 to 0.1 molality.

Determination of physical properties

Differential scanning calorimetry (d.s.c.). D.s.c. scans were obtained using samples weighing roughly 20 mg with a Perkin–Elmer DSC-4 instrument. Scans from room temperature to 150°C employed a heating rate of 10°C min^{-1}, and data were collected on samples quenched and rescanned under the same conditions. All scans were run under a dry nitrogen atmosphere. The glass transition temperature (T_g) was defined as one-half the total change in heat capacity (C_p) occurring over the transition region.

Dynamic mechanical thermal analysis (d.m.t.a.). Dynamic mechanical properties of the polyblends were determined using a Polymer Laboratories d.m.t.a. instrument. Sample dimensions for the extruded dog-bones were roughly 3 mm in width, 1.5 mm thick and 10 mm in length. Dimensions for the solvent-cast films varied so as to keep the calibration constant, $\log k$, between 3.5 and 4 while running in single cantilever beam mode with a free length of 1 mm. All samples were run at a heating rate of 5°C min^{-1} and a frequency of 1 Hz.

Stress–strain testing. Tensile properties were measured at room temperature using an Instron Table Model TM-M at a cross-head speed of 1 mm min^{-1}. All samples had a gauge length of 13 mm, and solution-cast films had widths of 2.5 mm and variable thickness. The data reported are the average of at least seven samples. The Young's modulus was obtained from the tangent of the initial slope of the force vs. elongation curve.

Scanning electron microscopy (s.e.m). Freeze-fractured surfaces were observed using an AMR 900 scanning electron microscope. In order to prevent charging, the samples were coated with 100 Å of gold-palladium. Samples were then observed at magnifications ranging from 500 to 5000 times.

Stereology.* S.e.m. micrographs were analysed by measuring the dimensions of statistically sampled section images using superimposed grids or test lines. Measured quantities, such as point fractions, intercept and feature counts, were related to structural quantities, such as volume fraction (or volume percentage), surface area per unit volume, and diameters.

RESULTS AND DISCUSSION

Sample preparation and structure

Sample preparation. Solution casting has been applied previously to the crosslinking of lignin derivatives with diisocyanates[16]. This method takes advantage of the mutual solubility of network components and catalyst in a solvent that evaporates prior to and during the crosslinking reaction. This evaporation is so slow as to

*Stereology refers to the quantitative characterization of microstructures, a procedure that involves the application of geometrical–statistical techniques and equations relating measurements on two-dimensional sections to three-dimensional structural quantities[15]

ensure phase equilibrium of all components at all times. Depending on mutual miscibility and solubility, distinct phases or domains in varying dimensions are established[17,18]. This method was adopted for the preparation of solution-cast polyblends with PMMA. Two solvents, with similar solubility parameters but different capacities to form hydrogen bonds, were selected, and were removed at a rate that allowed the formation of domains, the size of which was solely the result of mutual immiscibility.

In addition to solution casting, blend components were mixed in the melt and injection moulded[14]. The rapid vitrification achieved with this method tends to 'lock' the two blend components in a randomly entangled (non-equilibrium) state or a state very similar to that of a highly mixed melt. This results in a closely associated interphase with increased polymer–polymer interaction.

Fractionation of lignin component. Fractionation of HPL according to molecular size was performed using a previously tested solution method[13]. The characteristics of three fractions produced (*Table 1*) indicate that molecular weights by g.p.c. increased from 1900 to 10 000 (M_n) and from 2300 to 33 000 (M_w). Results by v.p.o. were generally in good agreement with data by g.p.c. Molecular-weight determinations of lignin continue to pose difficulties, and these data should be viewed as relative[13,19–21]. The observed rise in T_g with molecular weight followed the Fox equation[22], and this is the subject of another report[13]. Since the chemical composition of HPL fractions has previously been found not to vary significantly with molecular weight[13], it was assumed that differences in chemical structure were not substantial.

Sample structure. Typical photomicrographs of PMMA (*Figure 1a*) can be characterized by regular parabolic structures with lines radiating from an area near the focus, regardless of method of preparation—solution casting or injection moulding. Blends of HPL and PMMA cast from chloroform and THF (*Figures 1b* and *c*, respectively) reveal a two-phase (immiscible) morphology regardless of solvent, weight fraction, or molecular weight. Extruded HPL/PMMA blends (*Figures 1d* and *e*) have a less obvious two-phase morphology, although they are far from miscible. In order to distinguish their morphology, the fracture surface was etched by treatment with methanol (a solvent for HPL and a non-solvent for PMMA). The resulting texture (*Figure 1e*) shows long, narrow striations indicative of phase separation. The substantial differences in morphology between solution-cast and injection-moulded blends are attributed to differences in the rate of vitrification.

Stereology, which is a geometrical–statistical technique for characterizing three-dimensional structures from two-dimensional sections[15], was used to calculate domain size and volume fraction occupied by domains. The results indicated that all blends, regardless of method of preparation, or of weight fraction of each component, or of molecular weight, exhibited a space (and thus volume) distribution that corresponded to the blend ratio within a margin of error of 5%.

The relationship between domain size and method of preparation, as well as molecular weight and volume fraction of HPL (*Figure 2*), reveals that domain size increases with both weight fraction and molecular weight of HPL. This is consistent with both solvents, but slope and magnitude of the relationship differed. The chloroform films had consistently greater domain dimensions than the THF films; and the injection-moulded blends showed striation widths that were smaller (and fairly independent of HPL molecular weight and weight fraction) than the domains of the THF films. This is an initial indication for differences in molecular interaction in relation to method of preparation. Since the solubility parameters of the two solvents, chloroform and THF, are almost identical (i.e. 9.3 and 9.1, respectively), the difference in hydrogen-bonding potential must be held responsible for the morphological difference observed. Injection-moulded blends display phenomena typical of materials that failed to reach thermodynamic phase equilibrium before vitrification.

Thermal characteristics

Differential scanning calorimetry (d.s.c.). Typical d.s.c. thermograms for solution-cast and injection-moulded HPL/PMMA blends (*Figure 3*) reveal two endotherms at 63 and 104°C corresponding to HPL and PMMA, respectively, in the initial scan (*Figure 3*, scan A), and single transitions at 104°C in the samples annealed above T_g (*Figure 3*, scan B). The two endotherms are caused by enthalpy relaxation, which occurs when a polymer is cooled from the melt, and when the rapid rise in viscosity as the polymer approaches T_g causes the polymer chains to freeze into non-equilibrium conformations[23,24]. The resulting glass leaves an excess free volume quenched into the system. By annealing at temperatures above the two T_g values, the respective endotherms are replaced with a single broad T_g. Considering the SEM results (which indicated immiscibility, and showed no signs of

Table 1 Characteristics of molecular-weight fractions of hydroxypropyl lignin

Fraction	Acetone/hexane ratio	Fraction of material (%)	T_g (°C)	Molecular weight	
				G.p.c. (DMF)	V.p.o. (DMF)
Low MW	0.8	40	30	$M_n = 1900$ $M_w = 2300$	$M_n = 1700$
Medium MW[a]	1.0	16	68	$M_n = 2300$ $M_w = 4800$	$M_n = 2100$
High MW	ppt.	20	105	$M_n = 10000$ $M_w = 33000$	NA[b]

[a] A second medium-MW fraction was collected in low (9%) yield at an acetone/hexane ratio of 2. This had a T_g of 87°C, and M_n and M_w values by g.p.c. of 3250 (2800 by v.p.o.) and 5900, respectively

[b] Beyond the limit of accuracy for this procedure

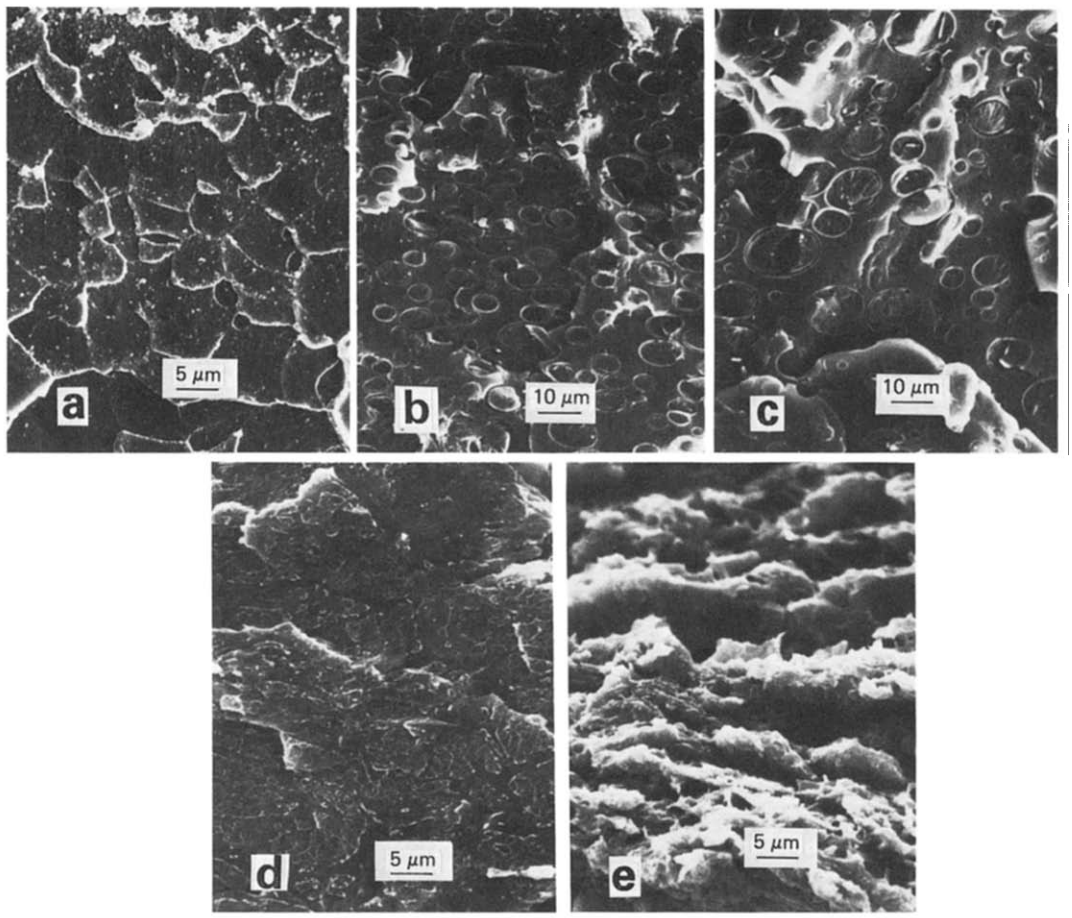

Figure 1 Scanning electron micrographs of (freeze) fracture surfaces of 25% HPL/PMMA blends: (a) PMMA (control); (b) blend cast from chloroform solution; (c) blend cast from THF solution; (d) injection-moulded blend (unetched); (e) injection-moulded blend (etched with methanol)

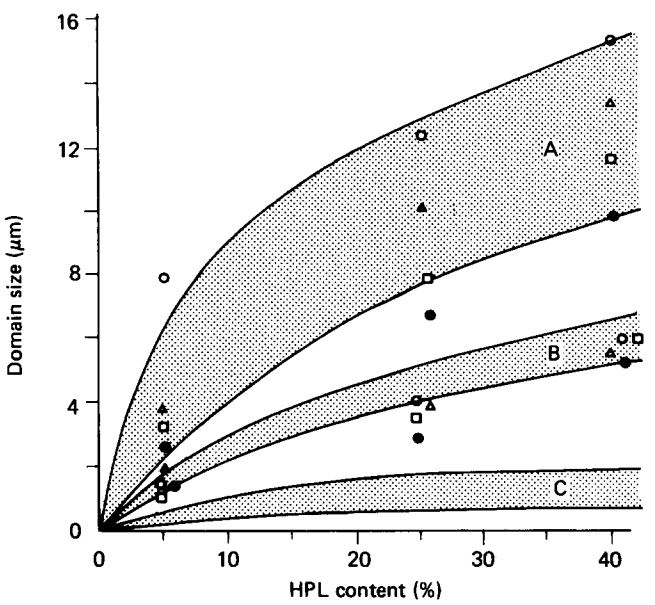

Figure 2 Relationship between domain size and HPL content for: A, chloroform solution-cast blends; B, THF solution-cast blends; C, injection-moulded blends (estimated). Symbols indicate unfractionated HPL (△), low-MW HPL (●), medium-MW HPL (□) and high-MW HPL (○)

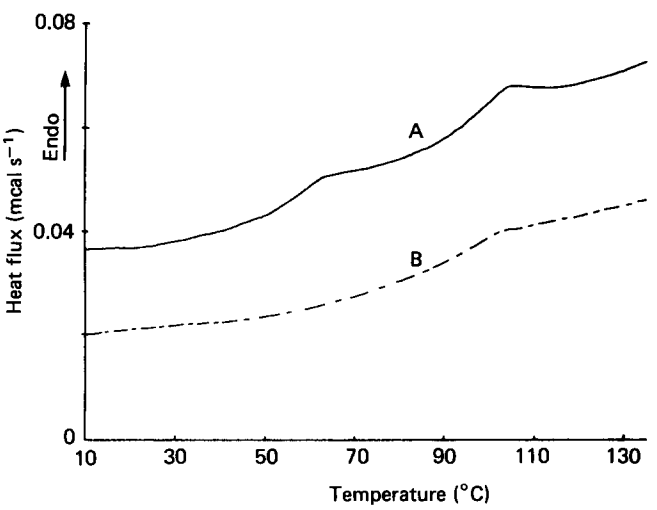

Figure 3 D.s.c. thermograms of THF solution-cast 40% medium-MW HPL/PMMA blend; A, initial scan; B, second scan

interaction between the two phases), the presence of a single T_g cannot be taken as an indication of phase uniformity[25]. Rather, this broad T_g, which in the case of low-molecular-weight HPL spans a range of 90°C, is believed to be the result of 'transitional smearing'. This phenomenon has previously been observed with blend components that have T_g values within ~20°C of each other[26], and it simply represents the overlapping of two T_g to produce a single broad T_g. If the point where the d.s.c. curve deviates from the baseline is considered as T_{g1}, and T_{gf} is the point after the endotherm where the d.s.c. curve returns to the baseline, then ΔT_g can be defined as:

$$\Delta T_g = T_{gf} - T_{g1} \quad (1)$$

For most polymers a sharp transition ($\Delta T_g < 15$°C) is

typical of a homogeneous material. This implies heterogeneities of < 50 to 100 Å[27], at least on the scale of thermal measurements. A broad transition, on the other hand, suggests a somewhat less than homogeneous blend. MacKnight has described compatible blends as those exhibiting a sharp transition, and less compatible blends as those having a wider, broader transition. The extreme case of a totally incompatible material is indicated by two separate transitions, signifying little attraction of one component for another[28].

The T_g values of HPL/PMMA blends (*Table 2*) indicate that the single T_g observed after annealing remains widely insensitive to HPL content (although sometimes fluctuating erratically) in all solution-cast blends, and that the PMMA transition is almost 20°C below that of the injection-moulded samples. The melt-mixed samples show T_g values that decline significantly with HPL content, and this decline varies in rate with HPL molecular weight. This sensitivity resembles a partially miscible system.

Dynamic mechanical thermal analysis (d.m.t.a.). The tan δ peak of d.m.t.a. thermograms provides a second measurement of T_g. The temperature vs. tan δ and storage modulus (log E') curves for pure PMMA (*Figure 4*) are typical for PMMA. The α or glass transition appears at 112°C for the moulded samples, and at 108 and 104°C for the THF- and chloroform-cast samples, respectively. T_g variations may be attributed to frequency effects[29]. A β transition, which is centred around 20–50°C, is generally

Table 2 Thermal analysis data of HPL/PMMA blends

Sample	HPL content (%)	Type of transition		T_g[c] (°C)	Breadth of T_g[c] (°C)	Onset of α transition (°C)
		Number[a]	Shoulder[b]			
Solution cast ($HCCl_3$)						
PMMA (control)		1	no	87.5 (104)	43 (15)	68
Unfractionated HPL	5	1	no	87 (107)	45 (34)	60
	25	2	no	90 (106)	45 (37)	60
	40	2	yes	74 (106)	63 (37)	54
Low-MW HPL	5	1	no	84.5 (100)	30 (30)	60
	25	2	yes	82 (100)	49 (30)	30
	40	2	yes	80 (96)	75 (32)	32
Medium-MW HPL	5	1	no	74 (99)	58 (33)	55
	25	2	no	87.5 (99)	50 (34)	45
	40	2	yes	80 (105)	70 (31)	50
High-MW HPL	5	1	no	80.7 (94)	30 (39)	55
	25	1	no	85 (98)	38 (34)	63
	40	1	no	84 (110)	27 (36)	60
Solution cast (THF)						
PMMA (control)		1	no	93 (108)	36 (22)	68
Unfractionated HPL	5	1	no	94 (103)	38 (28)	70
	25	2	no	91 (101)	48 (25)	73
	40	2	yes	89 (99)	62 (24)	72
Low-MW HPL	5	1	no	88 (115)	50 (27)	75
	25	2	yes	91 (110)	51 (25)	52
	40	2	yes	86 (102)	50 (22)	55
Medium-MW HPL	5	2	no	97 (110)	53 (34)	70
	25	2	yes	95 (110)	61 (28)	55
	40	2	yes	87 (104)	59 (27)	50
High-MW HPL	5	1	no	98 (107)	27 (29)	66
	25	2	no	110 (118)	28 (30)	75
	40	2	no	108 (116)	26 (25)	70
Injection moulded						
PMMA (control)		1	no	109 (112)	27 (24)	77
Unfractionated HPL	5	1	no	112 (118)	36 (22)	70
	25	2	no	99 (111)	55 (27)	65
	40	2	yes	98 (105)	57 (32)	50
Low-MW HPL	5	1	no	102 (119)	82 (22)	75
	25	2	yes	91 (99)	53 (28)	52
	40	2	yes	70 (90)	60 (36)	29
Medium-MW HPL	5	1	no	108 (113)	46 (23)	75
	25	2	yes	93 (102)	55 (33)	55
	40	2	yes	90 (99)	52 (31)	46
High-MW HPL	5	1	no	112 (118)	36 (21)	85
	25	2	no	103 (118)	60 (27)	70
	40	2	no	116 (122)	33 (27)	70

[a] During first temperature scan
[b] On α transition
[c] By d.s.c.; numbers by d.m.t.a. are given in parentheses

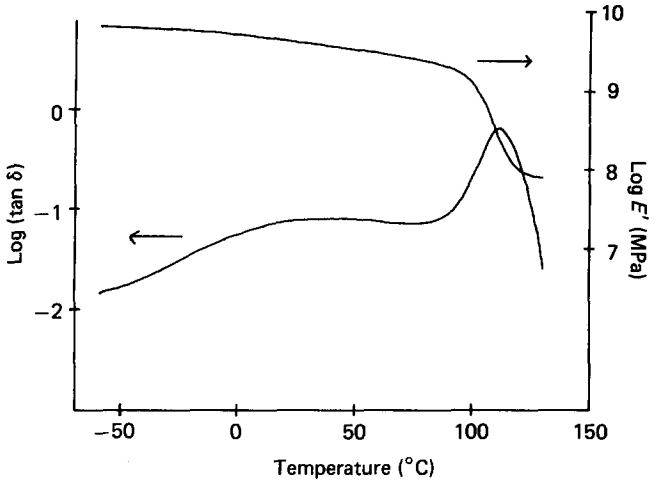

Figure 4 D.m.t.a. thermograms of PMMA control

attributed to rotation of the methyl ester side group[30]. The log E' curve remains relatively constant up to a temperature that correlates to the onset of the α transition. Since modulus measurements by d.m.t.a. are highly sensitive to the stability of sample dimensions, absolute log E' values are questionable and tan δ is emphasized instead.

The effects of increasing HPL content and of increasing molecular weight on the shape of the log E' and the tan δ curves (*Figures 5a–c*) indicate that the basic shape of the α transition remains unchanged with the addition of 5% low-MW HPL. However, with the addition of 25% HPL, considerable changes occur. The onset of the α transition is shifted from 80°C for pure PMMA to 60°C for the 25% HPL/PMMA moulded blend. The transition is also noticeably broader. The addition of 40% low-MW HPL causes the onset temperature of the α transition to be shifted to 30°C, some 50°C below that for pure PMMA. The shape of the α transition is extremely broad and the development of a shoulder becomes apparent. This broadening of the α transition and the onset of a shoulder is an indication of an immiscible system.

A rise in medium-MW HPL content causes blends to exhibit α-transition changes similar to those found with low-MW HPL (*Figure 5b*). No change is observed at an HPL content of 5%, and the α transition broadens, with the addition of 25 and 40% HPL. The onset of a reduction in log E' is shifted from 80°C to 60 and 55°C for the 25 and 40% HPL/PMMA blends, respectively. In addition, a faint shoulder appears on the low-temperature side of the α transition. Both observations indicate two-phase morphology. Plasticization is suggested where the onset temperature for the α transition is reduced without any indication of a separate T_g representing a second material component. This is the case for the 25% HPL/PMMA blend.

D.m.t.a. thermograms of moulded blends with high-MW HPL (*Figure 5c*) reveal more moderate degrees of tan δ peak broadening and shifting as compared with the corresponding lower-molecular-weight fractions of HPL. Peak maxima, and thus T_g, are observed consistently at higher temperatures than parent PMMA. This, and failure to result in distinct T_g separation and peak broadening, is an indication of antiplasticization. It can thus be concluded that HPL fails to produce two distinct tan δ (and T_g) maxima reflecting two polymer components; and that low-molecular-weight HPL plasticizes and high-molecular-weight HPL antiplasticizes PMMA. This suggests somewhat greater-than-expected compatibility between the two polymers.

The β transition (at ~20–50°C, *Figure 4*) is the result of methyl ester side-group rotations. Environmental changes, such as interactions with another polymer, can be expected to affect this secondary transition. Very slight decreases in β-transition magnitudes are noticed as HPL levels increase in all cases. However, this is believed to be the result of a decrease in the concentration (i.e. dilution) of methyl ester functional groups rather than in secondary interactions. In this case, the rotation of the methyl ester group would be reduced, resulting in a reduction of the log E''/log E' ratio (tan δ). However, no such reduction is observed.

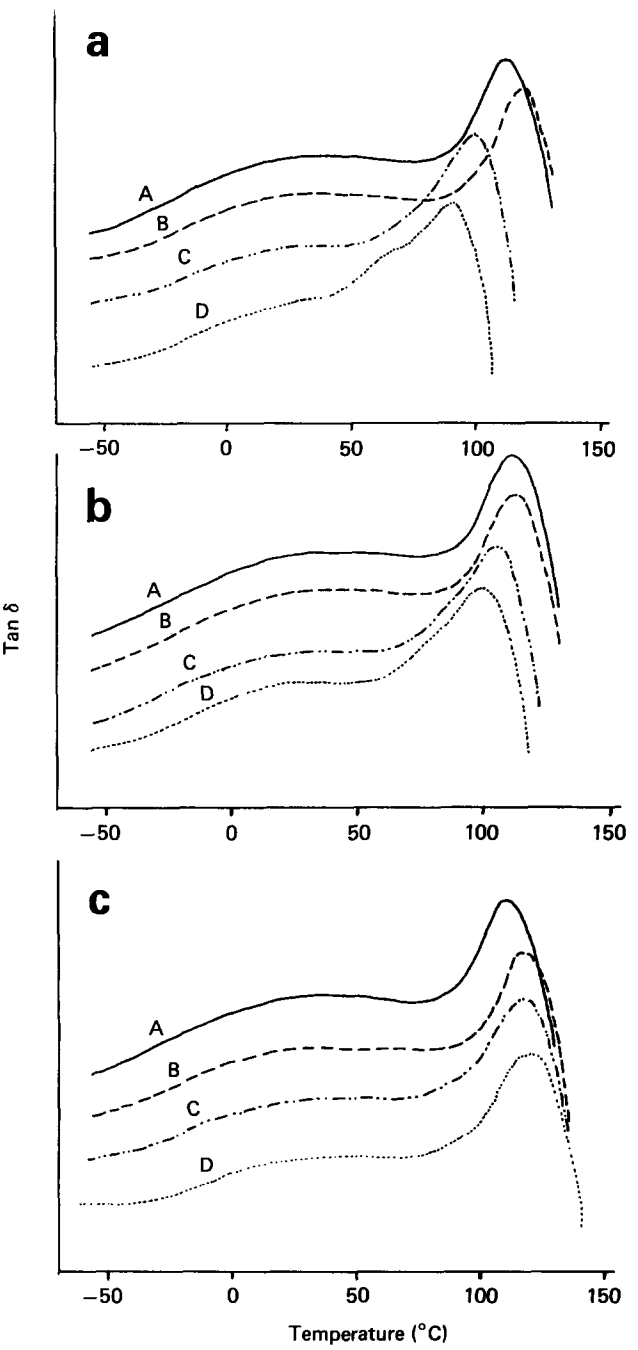

Figure 5 D.m.t.a. thermograms of HPL/PMMA blends: (a) low-MW HPL; (b) medium-MW HPL; and (c) high-MW HPL. Individual curves are for: A, PMMA (control); B, 5% HPL/PMMA blend; C, 25% HPL/PMMA blend; and D, 40% HPL/PMMA blend

Solution-cast blends showed d.m.t.a. thermograms with identical shapes to those obtained by injection moulding with respect to peak broadening and shoulder development; however, actual onset temperatures and α-transition position varied. A complete summary of the onset temperatures, T_g values (d.m.t.a., d.s.c.) and other thermal properties is found in *Table 2*. As with the d.s.c. data, a single T_g (α transition) was observed in all d.m.t.a. scans. T_g values for solution-cast blends were relatively independent of HPL content. No change exceeding 5°C was observed with any sample. The fact that the blend T_g is independent of HPL content indicates that an immiscible, phase-separated system is present and no interactions between blend components are occurring. Therefore it is suspected that the α transition represents that of uninhibited PMMA. Slight changes in the α transition of blends are due to the overlapping of a second T_g, that of HPL, which is seen as a low-temperature shoulder in *Figure 5*.

The injection-moulded samples produce consistently reduced T_g values with HPL content rising beyond 5%, except for high-MW HPL. Blends with 5% HPL content, and blends with high-MW HPL, have T_g values above that of the parent PMMA. Such a rise in T_g, above that of the parent polymers, is rare in polyblends, but it has been reported with other blended systems[31,32]. This phenomenon can be explained by polymer–polymer interactions that act as quasi-crosslinks, or by the process of injection moulding in which the blend polymers are 'locked' into non-equilibrium conformations that have less free volume and thus higher T_g values. This phenomenon is recognized as antiplasticization. No indications are observed in HPL/PMMA blends for the presence of strong polymer–polymer interactions.

Mechanical properties

When a polymer blend forms a single-phase material, its modulus of elasticity becomes roughly intermediate between that of the two parent polymers. On the other hand, when two polymers exist in separate phases, the relationship between composition and modulus is not nearly as simple. In one view, the structure that comprises the larger volume fraction should form the continuous phase and play the primary role in determining mechanical properties. The role of the secondary phase will be dictated by the interphase between the continuous (matrix) and the discontinuous (domain) phases. In other words, the degree of miscibility and the extent of interfacial adhesion govern the ultimate mechanical performance of a blend in the solid state.

S.e.m. and (a part of) thermal analysis (results) of HPL/PMMA blends have indicated two-phase morphology. Differences have been observed by s.e.m. between solution-cast and injection-moulded blends in terms of their domain–matrix interphase. Whereas the interphase of solution-cast blends (*Figures 1a–c*) suggests that the HPL domains act as filler, the morphology of injection-moulded blends does not reveal domain–matrix separation. Better association at the interphase is therefore indicated. Interfacial association suggests that HPL is more actively involved in the mechanical properties of the injection-moulded blends.

The change in Young's modulus with HPL content for injection-moulded HPL/PMMA blends (*Figure 6*) can be compared to values predicted by the rule of mixing[33]:

$$E_c = E_1 V_1 + E_2 V_2 \quad (2)$$

where E_c is the modulus of the blend, $E_{1,2}$ are the moduli of components 1 and 2, and $V_{1,2}$ are the volume fractions of components 1 and 2. The results show that injection-moulded blends containing 5% HPL (of any molecular weight) have a larger increase in modulus than predicted by the model (*Figure 6*). (Solution-cast blends are not shown since their values varied inconsistently probably due to the presence of large domains, which act as crack

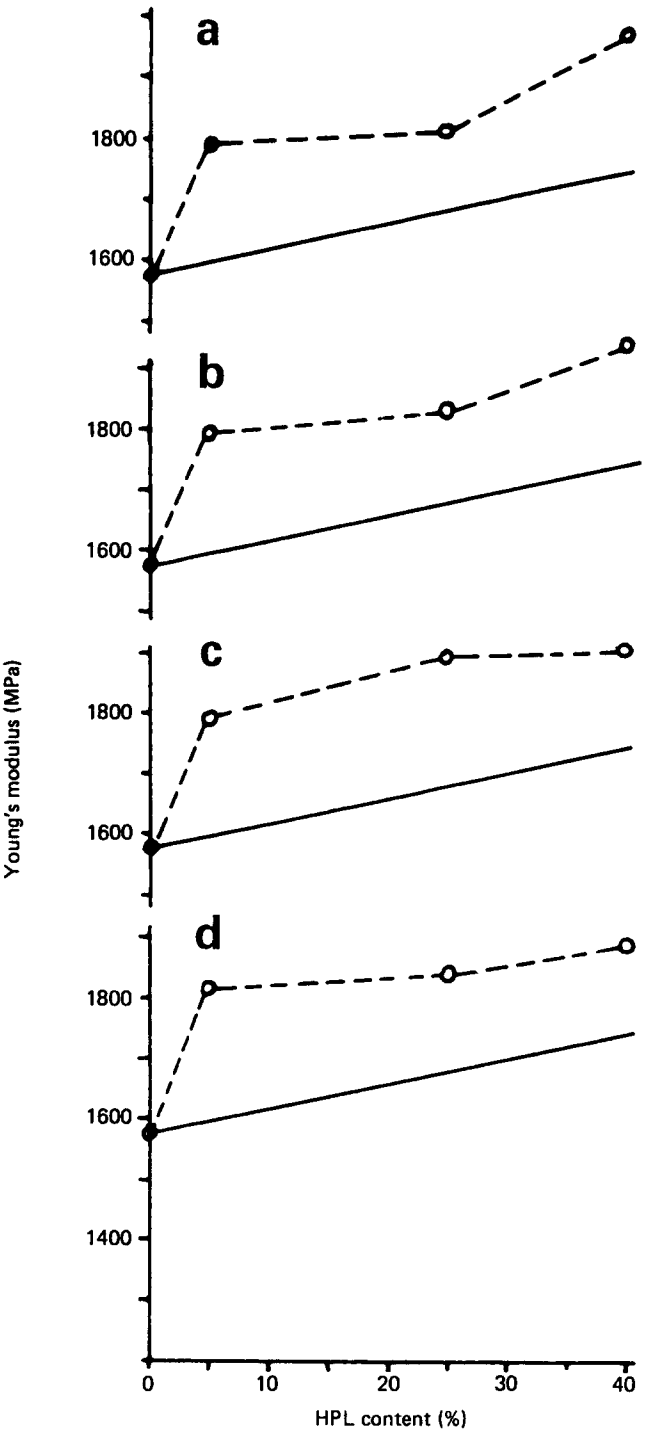

Figure 6 Relationship between Young's modulus and HPL content for injection-moulded HPL/PMMA blends (broken line) and theory (i.e. equation (2)) (full line): (a) unfractionated HPL; (b) low-MW HPL; (c) medium-MW HPL; and (d) high-MW HPL

propagation sites and reduce the true cross-sectional area of the sample.) At 25 and 40% HPL the injection-moulded blends showed increases in modulus that corresponded to the gains predicted by equation (2). The fact that the moduli of injection-moulded blends containing 5% HPL were consistently higher than predicted indicates that the high-modulus HPL (i.e. 2000 MPa)[34] interacts more actively with the matrix polymer than is suggested by a simple weighted average. This agrees with T_g results, which provided some indication for polymer–polymer interaction.

Since lignin is a high-modulus (glassy) material it would not be considered a (tensile) strength builder. This is verified for solution-cast and injection-moulded samples (*Figure 7*), which all reflect noticeable decreases in tensile strength with increasing HPL content. However, no dependence on molecular weight is detected.

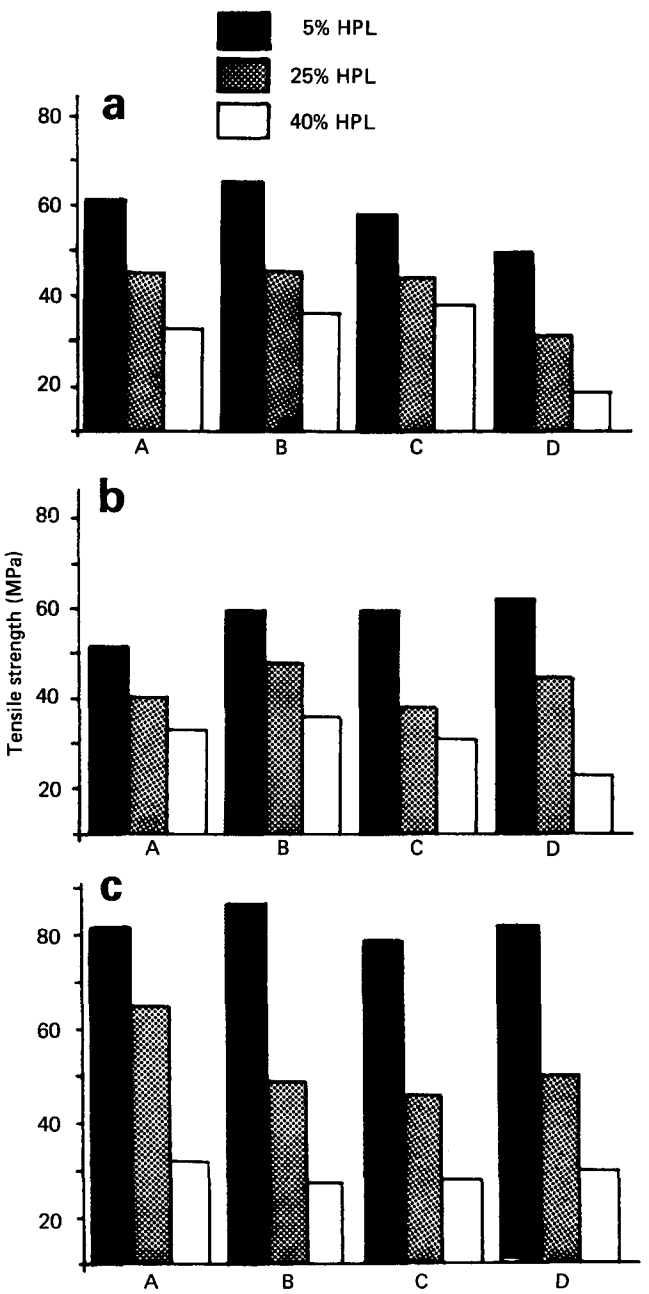

Figure 7 Tensile strength data for HPL/PMMA blends: (a) chloroform solution-cast; (b) THF solution-cast; and (c) injection-moulded. The HPL used is as follows: A, unfractionated HPL; B, low-MW HPL; C, medium-MW HPL; D, high-MW HPL

Injection-moulded blends had higher tensile strengths than those produced by solution casting, especially at 5 and 25% HPL levels. This may be taken again as a sign of superior morphology, or of polymer–polymer interaction as suggested by s.e.m., d.s.c. and d.m.t.a.

The ultimate strain of HPL/PMMA blends was found to decline with rising HPL content in accordance with tensile strength data. This decrease was again independent of HPL molecular weight, and injection-moulded samples were again superior to those cast from solution, especially at 5 and 25% HPL contents. This provides further support for the notion that polymer–polymer interaction plays some role in the injection-moulded blends.

CONCLUSIONS

Blends of PMMA and various molecular-weight HPLs produced two-phase material systems. Domain dimensions varied with method of preparation (i.e. solution casting and injection moulding) and solvent type. Enthalpy relaxation was responsible for two endothermic transitions in the initial d.s.c. thermogram, and a single, broad transition was observed in all second scans and in d.m.t.a. thermograms. This transition was centred at lower or higher temperatures than that representing the T_g of pure PMMA, and this was attributed to plasticization and antiplasticization. This suggests some degree of polymer–polymer interaction and compatibility.

Analysis of the β transitions by d.m.t.a. indicated that polymer–polymer interactions involving the carbonyl (and methoxy) group of PMMA did not occur.

The interphase between the domains and the matrix differed with respect to blend preparation. Solution-cast blends showed domains that were pulled away from the matrix whereas the injection-moulded blends showed HPL striations that were closely associated with the matrix. The fast rate of vitrification by the injection-moulding process appears to have locked the polymers in a randomly mixed state whereas the slower rate of vitrification for the solution-cast blends allowed domains of large dimensions to form.

The addition of HPL to PMMA resulted in an increase in modulus. A very large initial increase was observed with 5% HPL, and further increases were recorded with 25 and 40% HPL. The rate of modulus rise between 5 and 40% closely followed the rule of mixtures. This supports the contention that HPL contributes to the material properties of the blend via some type of polymer–polymer interaction.

Ultimate properties, tensile strength and ultimate strain, decreased with the addition of HPL to PMMA. Injection moulding produced superior material properties.

Variations in the molecular weight of HPL had no significant effect on the material properties of HPL/PMMA blends.

ACKNOWLEDGEMENTS

Valuable assistance was provided by Dr S. S. Kelley and Dr T. G. Rials, and this is gratefully acknowledged. Financial support was provided by the National Science Foundation under Grant Number CBT-8512636.

REFERENCES

1 Platzer, N. A. J. (Ed.), 'Multicomponent Polymer Systems', Adv. Chem. Ser. 99, American Chemical Society, Washington DC, 1971
2 Han, C. D. (Ed.), 'Polymer Blends and Composites in Multiphase Systems', Adv. Chem. Ser. 206, American Chemical Society, Washington DC, 1984
3 Walsh, D. J., Higgins, J. S. and Maconnachie, A. (Eds.), 'Polymer Blends and Mixtures', NATO ASI Series E, Applied Sciences, No. 89, Nijhoff, The Hague, 1985
4 Shaw, M. T. *Polymer Eng. Sci.* 1982, **22**(2), 115
5 Paul, D. R. and Barlow, J. W. *J. Macromol. Sci.–Rev. Macromol. Chem.* 1980, **C18**, 109
6 Pavan, A., Ricco, T. and Rink, M. *Mater. Sci. Eng.* 1980, **45**, 201
7 Pavan, A., Ricco, T. and Rink, M. *Mater. Sci. Eng.* 1981, **48**, 9
8 Cooper, G. D. and Katchman, A. US Patent 4 389 511 (1983)
9 Wellinghoft, S. T., Koenig, J. L. and Baer, E. *J. Polym. Sci., Polym. Phys. Edn.* 1977, **15**, 1913
10 Paul, D. R. Ch. 1 in ref. 3
11 Rudin, A. 'The Elements of Polymer Science and Engineering', Academic Press, New York, 1982, Ch. 12
12 Wu, L. C.-F. and Glasser, W. G. *J. Appl. Polym. Sci.* 1984, **29**, 1111
13 Kelley, S. S., Ward, T. C., Rials, T. G. and Glasser, W. G. in preparation
14 Maxwell, B. *SPE J.* 1972, **28**(2), 24
15 Underwood, E. E. 'Quantitative Stereology', Addison-Wesley, Reading, MA, 1970
16 Saraf, V. P. and Glasser, W. G. *J. Appl. Polym. Sci.* 1984, **29**, 1831
17 Saraf, V. P., Glasser, W. G., Wilkes, G. L. and McGrath, J. E. *J. Appl. Polym. Sci.* 1985, **30**, 2207
18 Saraf, V. P., Glasser, W. G. and Wilkes, G. L. *J. Appl. Polym. Sci.* 1985, **30**, 3809
19 Sarkanen, S., Teller, D. C., Hall, J. and McCarthy, J. L. *Macromolecules* 1981, **14**, 426
20 Lange, W., Faix, O. and Beinhoff, O. *Holzforsch.* 1983, **37**, 63
21 Pellinen, J. and Salkinaja-Salonen, M. *J. Chromatogr.* 1985, **328**, 299
22 Fox, T. G. *Bull. Am. Phys. Soc.* 1956, **1**, 123
23 Hatakeyama, T., Nakamura, K. and Hatakeyama, H. *Polymer* 1982, **23**, 1801
24 Rials, T. G. *J. Wood Chem. Technol.* 1984, **4**(3), 331
25 Karasz, F. E. Ch. 2 in ref. 3
26 Gardlund, Z. G. in ref. 2, Ch. 9
27 Turi, E. A. *et al.*, 'Thermal Characterization of Polymer Materials', Academic Press, New York, 1981, p. 881
28 MacKnight, W. J., Karasz, R. E. and Fried, J. R. in 'Polymer Blends', (Eds. D. R. Paul and S. Newman), Academic Press, New York, 1978, pp. 224–228
29 Kwei, T. K. *J. Appl. Polym. Sci.* 1984, **22**, 307
30 McCrum, N. G., Read, B. E. and Williams, G. 'Anelastic and Dielectric Effects in Polymer Solids', Wiley, New York, 1967
31 Pennacchia, J. R., Pearce, E. M., Kwei, T. K., Bulkin, B. J. and Chen, J. P. *Macromolecules* 1985, **20**, 50
32 Gordon, M. and Taylor, J. S. *J. Appl. Chem.* 1952, **2**, 493
33 Sheldon, R. P. 'Composite Polymeric Materials', Applied Science, New York, 1982, p. 75
34 Falkehag, S. I. *Appl. Polym. Symp.* 1975, **28**, 247